

# Software-based Real-time Full-duplex Relaying: An Experimental Study

Muhammad Sohaib Amjad *Student Member, IEEE* and Falko Dressler *Fellow, IEEE*

**Abstract**—Relaying in wireless networks is one of the most important concepts to improve the overall communication performance and to increase coverage. Relay systems can work in either half or full-duplex mode. Half-duplex relaying unfortunately increases the overall latency and also causes spectral losses. On the other hand, in-band full-duplex relaying helps to overcome such issues by simultaneously receiving packets from the source and forwarding them towards the destination. We present a software-based real-time full-duplex relaying system, which we implemented in GNU Radio. The system supports running simulations using an abstract channel model as well as over-the-air experiments using Software Defined Radios (SDRs). A major challenge in developing such a system is dealing with self-interference. For this, we constructed a new looped self-interference cancellation system and integrated it with the GNU Radio implementation. In an experimental study, we validated and evaluated our system to characterize the practical performance of the proposed full-duplex relay system. Our main focus is on the impact of the residual looped self-interference, for which we show analytical and simulation results to confirm the experimental study.

**Index Terms**—Full-duplex relays, half-duplex relays, looped self-interference, OFDM, decode and forward relaying strategy, capacity gain, active cancellation, passive suppression.

## I. INTRODUCTION

The highly complex and unpredictable channel conditions can cause severe degradation of a wireless signal, which as a result has a significant impact on the performance of a wireless system. The amount of Signal-of-Interest (SoI) depreciation while traveling from source to destination, sets the basis for the following decoding errors at the destination, and this not only affects the data rate but also the coverage area of a wireless system. For instance, in a highly degrading wireless channel, we can increase the coverage area of a wireless system at the cost of lower data rates along with the possible risk of losing the communication entirely, or reduce the coverage region (decreasing the cell size) to maintain the high data rates, which means more equipment. In recent years, to overcome this capacity vs. coverage dilemma, infrastructure relays have been utilized and even employed by the wireless standards such as 3GPP LTE [1] and WiMAX [2], as they can greatly improve the system capacity and expand the coverage of a wireless network at the same time.

Nevertheless, these infrastructure relays operate in HD mode, which means they require additional resources typically in the time domain for reliable communication. As illustrated

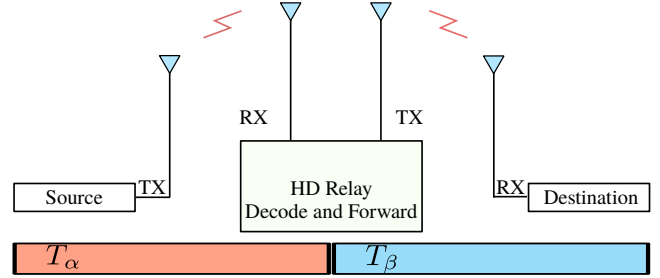


Figure 1. A standard two-hop relay system operating in Half-Duplex mode.

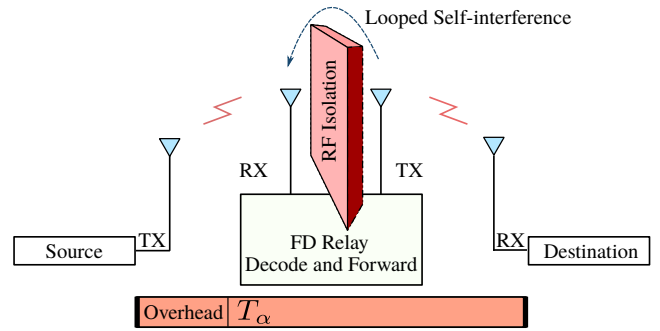


Figure 2. A two-hop relay system operating in Full-Duplex mode.

in Figure 1, a two-hop Time Division Duplex (TDD)-based Half-Duplex Relay (HDR) receives the data from a source in time slot  $T_\alpha$ , and then waits to retransmit the data towards a destination in the next available time slot  $T_\beta$ , where the waiting time depends on the implemented relaying strategy (i.e., Amplify and Forward (AF) or Decode and Forward (DF) scheme). The deployment of typical HDRs in a network increases the end-to-end latency (with such TDD-based relays) and causes spectral losses (as in Frequency Division Duplex (FDD)-based relays), in addition to inefficient channel utilization.

In the past few years, a substantial amount of research has been done on in-band FD wireless systems [3]. Several works [4]–[11], presented different techniques and architectures to address the prime factor impeding FD wireless communications, namely the Self-Interference (SI), which primarily arises due to radio's own transmission at the same time and frequency. Yet, while FD communications has gained most attention with substantial volume of literature available, covering both theoretical and experimental works; full-duplex relaying is still an under-explored topic, with most of the existing studies based on analytical models only.

M. Sohaib and F. Dressler are with Heinz Nixdorf Institute and Dept. of Computer Science, Paderborn University, Germany, e-mail: {amjad,dressler}@ccs-labs.org.

A Full-Duplex Relay (FDR) system can simultaneously receive from the source and forwards towards the destination, as illustrated in Figure 2. This necessarily improves the spectral efficiency of FDD-based relays, and considerably reduces the end-to-end delay in TDD-based relay systems, especially in a multi-hop network. In addition, depending on the implemented relaying scheme (the two most widely adopted techniques are AF and DF), there can be a marginal increase in the latency due to additional processing at the relay node. However, this is still significantly smaller compared to what HDR systems offer.

To achieve optimal performance with FDRs, the mitigation of Looped Self-Interference (LSI) is the fundamental requirement. For maximal suppression of LSI, usually, both passive suppression and active cancellation techniques are employed. Passive suppression typically requires the isolation of strong direct/leaked SI component to avoid the saturation of Analog-to-Digital Converters (ADCs) in the received signal processing path, and it is usually done via antenna separation and Balun transformer, or through an RF coupler. Whereas, active cancellation can be done in the analog domain via RF cancellation circuitry, and in the digital domain by modeling an equivalent discrete system capturing the channel effects. Any residual LSI after these self-interference suppression stages basically reduces the Signal-to-Interference-plus-Noise Ratio (SINR) of the SoI, which consequently decreases the overall system performance and reduces the throughput gain.

Extending our work in [12], which presents the first implementation of a General Purpose Processor (GPP)-based DF-FDR in GNURadio<sup>1</sup> for use with Software Defined Radios (SDRs) as well as in simulation mode; and compares its practical performance with conventional half-duplex DF relays. In this extension of the original conference paper, we give more insights into the underlying models as well as the implementation and also added a completely new section using the developed framework in simulation mode to validate the results. Our FD relay system includes the implementation of a novel real-time LSI cancellation block in the GNU Radio framework for the elimination of self-interference in the digital domain, and a simple RF isolation technique for passive suppression. We are now going to make the code available as Open Source given the positive feedback from the community. In our first performance evaluation, we study the Packet Delivery Ratio (PDR) in simulations as well as with real-world experiments, and the achievable throughput gains in both FD and HD modes. Our results demonstrate and underline the huge advantage of switching from the classical half-duplex relaying to full-duplex relay systems.

Our main contributions can be summarized as follows:

- We present a real-time OFDM-based Decode and Forward FDR implementation, which allows to monitor the real-time LSI cancellation in both time and frequency domains.
- We show that when LSI is fully suppressed, the throughput gain of FDR (including the overhead) is nearly twice compared to classical HDR systems.

- We study the impact of residual LSI due to estimation error, both analytically and in the simulation environment, and present the channel capacity gain of FDR over HDR.
- We experimentally investigate the impact of residual LSI in real-time on the FDR performance and throughput, the noise floor for SoI, and the transmit power requirement of the source.
- Our open-source software solution for FD relaying utilizes GNU Radio for signal processing. This makes the implementation accessible to fellow researchers and allows easy modifications for the testing of new concepts.

## II. RELATED WORK

In the era of ever-growing wireless traffic and high-speed connectivity, the issue of coverage vs. data rates in a band-limited wireless link has gained significant attention. Infrastructure relays in this regard have effectively addressed the stated issue and have been adopted by many wireless standards. Nevertheless, due to their half-duplex nature, they do have added disadvantages like poor spectral usage and increased latency. The most commonly studied and employed relaying strategies include AF and DF schemes. In the literature, to overcome the added disadvantages of these relaying strategies due to their half-duplex nature, different works have considered approaches such as cooperative decoding for diversity gain [13], and two alternating relay nodes to mimic FD mode [14]. Nevertheless, these approaches have not been able to entirely compensate for the losses these HD relays incur.

In recent years, full-duplex relaying has been studied in quite detail, after-all, the implications of such relaying systems are qualitatively beneficial in terms of both spectral efficiency and network latency. However, most of the research conducted in the domain have presented their analytical findings and considered theoretical approaches to state the gains of FD relaying. For instance, in [15], the authors considered an AF relaying system with low-resolution ADC; and did analytical modeling of LSI and quantization noise to analyze the achievable spectral efficiency. Similarly, in [16] an analytical model has been employed based on Markov chain modeling to analyze the outage probability in FD multi-relay channels. Likewise, in [17] the optimal power allocation in DF based FDRs to effectively handle the residual LSI has been discussed. Other such works include [18], where the RF impairment effects such as nonlinear behavior of power amplifier have been analyzed; and [19], in which the impact of looped-back channel estimation error on the performance of AF-based FD relaying is studied. These studies and other similar works have mostly assumed (often implicitly) that the relay system has the full-duplex capability, and the LSI can be eliminated without any complication. As a result, they not only lack actual implementation perspective but also make strong assumptions on requirements such as synchronization of estimated LSI and actual LSI for effective real-time cancellation.

In [20], a complete FDR design, implementation, and performance evaluation have been presented. The work introduced an intelligent class of AF relays and named it as

<sup>1</sup><https://www.gnuradio.org/>

Construct and Forward (CF) relaying, which unlike the naïve forwarding done by a typical AF relay, forwards the relayed signal in such a way that it constructively adds up with the direct signal (coming from source) at the destination. In order to work effectively, the constructive filter used at the relay node requires the Channel State Information (CSI) of all four paths, i.e., S-R, R-R, R-D, and S-D, which is a complex task. Also, the proposed design is still based on AF relaying, and although CF avoids noise amplification by efficiently choosing the amplification factor, this also reduces the power levels of the relayed signal and compromises the system performance.

Apart from the contemporary full-duplex and half-duplex relay systems, an advance approach, i.e., buffer-aided relaying [21]–[23], for the general two-hop FD relay system is also proposed in the literature. The buffer-aided relaying approach adaptively selects either to receive, transmit, or both transmit and receive simultaneously, in a given time slot based on the quality of the self-interference channel. In [22], the overall throughput rates are shown to be improved with buffer-aided FD relaying as compared to conventional FD relaying but only under the assumption that there is residual LSI, and as long as source and destination nodes are in communication range. The work in [23], further maximizes the throughput of such buffer-aided FD relaying in fading channels. Nevertheless, these works are numerical and/or simulative studies under certain assumptions, and certainly, lack the perspective of practical performance and challenges.

Contrary to the mentioned works, this paper presents real-time GNURadio based implementation of an FDR with DF relaying scheme, which eliminates the noise amplification limitation of AF and CF-based FD relays. Additionally, the existing implementations are Field-Programmable Gate Arrays (FPGA)-based such as WARP Mango board [20], and while these FPGA-based SDRs offer deterministic timing and low latency, nevertheless, they are rather inflexible, and it is often challenging to implement complex signal processing algorithms in them. In-contrast, our proposed FDR implementation is GPP-based, build upon open-source platform GNURadio, which is easily accessible and most importantly, the signal processing is done in software, with high-level programming languages C++ and Python. Thus, making it particularly easy to use, modify, and debug.

### III. RELAYING SYSTEM MODEL

In this work, we consider a two-hop relay system with a source node, a destination node, and a relay node with Decode and Forward relaying scheme. The entire relay system operates in non-cooperative manners, and the packets from source cannot reach destination directly. Also, the relay node in-between source and destination can operate either in HD or FD mode. When the considered system operates in HD relaying mode, the relay node simply receives a packet from source in time slot  $T_\alpha$ , and forwards it to destination in time slot  $T_\beta$ , as shown in Figure 3a. However, when operating in full-duplex mode, the relay node first needs to suppress the LSI before moving towards the decoding part as illustrated in Figure 3b.

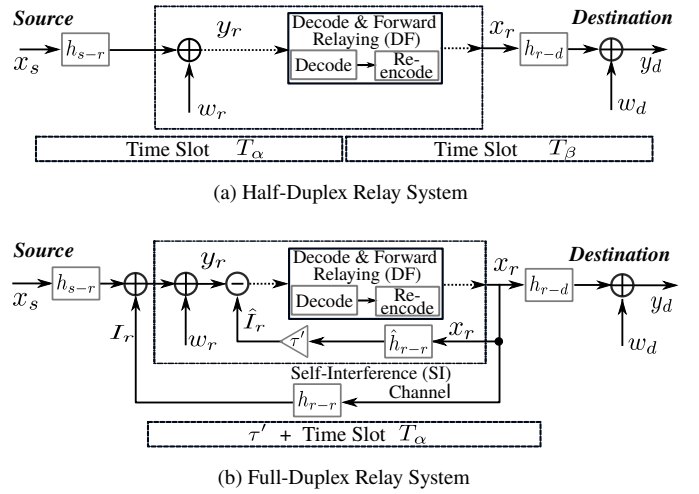


Figure 3. Block diagram of a two-hop relay system operating in half-duplex and full-duplex modes with DF relaying scheme.

#### A. Half-Duplex Mode

In the case of half-duplex relaying mode with Decode and Forward scheme, depicted in Figure 3a, a packet from the source node is first decoded at the relay node, it is then re-encoded and forwarded towards the destination. The received baseband samples  $y_r$  at the inputs of relay node, and the received samples  $y_d$  at the destination node can be written as

$$y_r[n] = x_s[n] * \bar{h}_{s-r} + w_r[n], \quad (1)$$

$$y_d[n] = x_r[n] * \bar{h}_{r-d} + w_d[n], \quad (2)$$

where  $x_s$  and  $x_r$  are the samples generated by source and relay nodes,  $w_r$  and  $w_d$  is the zero mean noise component at the relay and destination ends, and  $\bar{h}_{s-r}$ ,  $\bar{h}_{r-d}$  are the channel coefficients of source-relay and relay-destination channels, respectively. The instantaneous signal powers in Equations (1) and (2) can be obtained as  $E\{|x_s[n]|^2\} = P_s$  and  $E\{|x_r[n]|^2\} = P_r$ . Similarly, the noise powers at relay and destination ends can be computed as  $E\{|w_r[n]|^2\} = \sigma_r^2$  and  $E\{|w_d[n]|^2\} = \sigma_d^2$ .

From Equations (1) and (2), the instantaneous received Signal-to-Noise Ratio (SNR) at relay node ( $\gamma_r$ ) and destination node ( $\gamma_d$ ) can be computed as

$$\gamma_r = \frac{P_s \|h_{s-r}\|^2}{\sigma_r^2} \quad \text{and} \quad \gamma_d = \frac{P_r \|h_{r-d}\|^2}{\sigma_d^2}. \quad (3)$$

Since DF relaying scheme decodes and re-encodes each symbol, therefore, the instantaneous end-to-end SNR ( $\gamma_i$ ) can be calculated as

$$\gamma_i = \min \left\{ \frac{P_s \|h_{s-r}\|^2}{\sigma_r^2}, \frac{P_r \|h_{r-d}\|^2}{\sigma_d^2} \right\}, \quad (4)$$

i.e.,  $\gamma_r$  or  $\gamma_d$  whichever is the lowest, benchmarks the resultant decode and forward based HD relay performance.

#### B. Full-Duplex Mode

Now, when the relaying is done in FD mode, the relay node receives the samples  $y_r$  from sources, and simultaneously

forwards the processed samples  $x_r$  towards the destination. This results in looped-back self-interference, which is therefore required to be suppressed before feeding the samples  $y_r$  to the decoding blocks, as depicted in Figure 3b. Otherwise, the DF scheme will not be able to decode anything due to the LSI that appears as a result of simultaneous reception and forwarding.

The samples received at the input of a relay node after LSI suppression ( $y_{\text{res}}$ ) are obtained as

$$y_{\text{res}}[n] = x_s[n] * \bar{h}_{s-r} + w_r[n] + I_r[n - \tau'] - \hat{I}_r[n - \tau']. \quad (5)$$

In (5),  $I_r$  and  $\hat{I}_r$  are the actual and estimated looped-back SI samples, and  $\tau'$  is the delay incurred by the relay front end hardware and decoding processing in DF strategy. Note that if  $\tau'$  is not acquired correctly, then the subtraction of non-synchronized estimated LSI  $\hat{I}_r$  from looped-back SI  $I_r$ , can drive the system towards instability. The residual signal samples ( $y_{\text{res}}$ ) in (5) can be reformulated as

$$y_{\text{res}}[n] = x_s[n] * \bar{h}_{s-r} + w_r[n] + x_r[n - \tau'] * (\bar{h}_{r-r} - \hat{h}_{r-r}), \quad (6)$$

$$y_{\text{res}}[n] = x_s[n] * \bar{h}_{s-r} + w_r[n] + x_r[n - \tau'] * \bar{e}_{r-r}, \quad (7)$$

where  $\bar{h}_{r-r}$  and  $\hat{h}_{r-r}$  are the actual and estimated relay-relay channel coefficients (including both the impairments due to the front ends and multi-path environment), and  $\bar{e}_{r-r}$  is the error between actual and estimated coefficients.

Similarly, the received samples at the input of destination node ( $y_d$ ) are then obtained as

$$y_d[n] = x_r[n] * \bar{h}_{r-d} + w_d[n], \quad (8)$$

and the instantaneous signal power of the delayed samples at the relay end can be computed as  $E\{|x_r[n - \tau']|^2\} = P'_r$ .

Thus, by using Equations (7) and (8), the instantaneous received SNR at relay node ( $\gamma_r$ ) and destination node ( $\gamma_d$ ) can be computed as

$$\gamma_r = \frac{P_s \|h_{s-r}\|^2}{\sigma_r^2 + P'_r \|e_{r-r}\|^2}, \quad (9)$$

and

$$\gamma_d = \frac{P_r \|h_{r-d}\|^2}{\sigma_d^2}, \quad (10)$$

and like in DF-based half-duplex relaying, the instantaneous end-to-end SNR ( $\gamma_i$ ) in DF-based full-duplex relaying is obtained as

$$\gamma_i = \min \left\{ \frac{P_s \|h_{s-r}\|^2}{\sigma_r^2 + P'_r \|e_{r-r}\|^2}, \frac{P_r \|h_{r-d}\|^2}{\sigma_d^2} \right\}. \quad (11)$$

From the comparison of (4) and (11) it can be seen that unlike HD mode,  $\gamma_i$  in FD mode is also affected by the residual LSI, i.e.,  $P'_r \|e_{r-r}\|^2$  factor, and when  $\|e_{r-r}\|^2 = 0$ , which in-practice never happens, both HD and FD modes offer same end-to-end SNR ( $\gamma_i$ ).

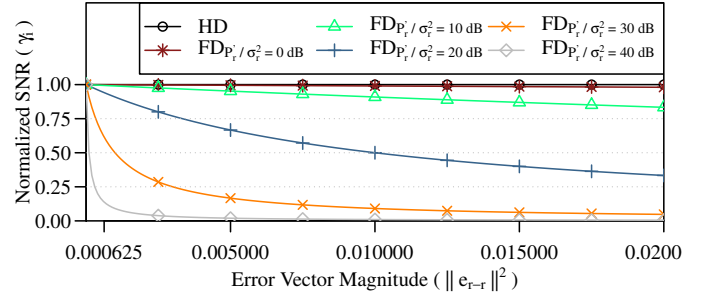


Figure 4. Instantaneous end-to-end SNR  $\gamma_i$  versus error vector magnitude  $\|e_{r-r}\|^2$  in both half-duplex and full-duplex modes for different  $P'_r/\sigma_r^2$ .

### C. Impact of Estimation Error on $\gamma_i$ in DF-based Relays

Unlike HD relaying, where the reception and forwarding are time separated, FD relaying innately suffers from LSI because of simultaneous reception and forwarding. In the case of equal transmit power of both source  $P_s$  and relay  $P_r$  nodes and under the assumptions of similar channel conditions (i.e.,  $\|h_{s-r}\|^2 \approx \|h_{r-d}\|^2$ ) and the receiver noise component (i.e.,  $\sigma_r^2 \approx \sigma_d^2$ ), Equation (11) can be reduced to

$$\gamma_i = \frac{P_s \|h_{s-r}\|^2}{\sigma_r^2} \left( \frac{1}{1 + \|e_{r-r}\|^2 P'_r/\sigma_r^2} \right), \quad (12)$$

where the prime SNR depreciating component in (11) under the assumptions is  $\|e_{r-r}\|^2 P'_r/\sigma_r^2$  factor. Thus, for optimal performance, the magnitude of estimation error plays a crucial role and has a direct relation with relay transmit power  $P_r$  at that instant. Notice that for  $\|e_{r-r}\|^2 = 0$ , both HD and FD relaying modes offer the same  $\gamma_i$ .

Figure 4 shows the impact of estimation error  $\|e_{r-r}\|^2$  on the received end-to-end SNR ( $\gamma_i$ ) at different transmit powers of the relay node. For simplicity, all the other parameters in (12) are either normalized or fixed. It can be seen in the plot that in comparison to HD relaying, the received SNR in FDR case starts decreasing with increasing  $\|e_{r-r}\|^2$ , and a precipitous drop in the SNR can be observed at higher power relay transmissions ( $P'_r/\sigma_r^2$ ). These numerical results clearly show the critical dependence of FDR performance on both estimation error magnitude and the relay node transmit power, where, in the presence of estimation error, a large transmit power at the relay end substantially depreciate the end-to-end SNR  $\gamma_i$ .

From Equations (4) and (12), the channel capacity gain of FDR over HDR  $C_{\text{FD}}/C_{\text{HD}}$  can be computed as

$$C_{\text{FD/HD}} = 2 \cdot \log_2 \left( 1 + \frac{1}{1 + \|e_{r-r}\|^2 P'_r/\sigma_r^2} \right), \quad (13)$$

where the factor of "2" in (13) is there because of the simultaneous reception and forwarding capability of FDRs. Figure 5 demonstrates the impact of estimation error  $\|e_{r-r}\|^2$  on the channel capacity gain at different transmit power levels of the relay end. From the comparison of Figures 4 and 5, it can be observed that even-though the SNR drops in FDR until certain error magnitudes are quite high as compared to HDR, nevertheless, the channel capacity gain of FDR over HDR is

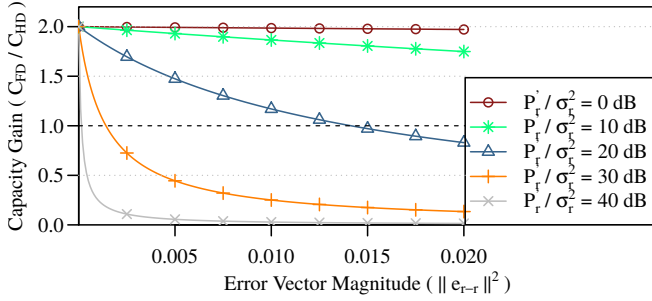


Figure 5. Channel capacity gain of FDRs over HDRs against increasing error vector magnitude  $\|e_{r-r}\|^2$  for different  $P'_r/\sigma_r^2$ .

still significantly better. This numerical finding particularly asserts the advantage of FD relaying over classical HDR systems.

#### IV. LOOPED SELF-INTERFERENCE SUPPRESSION

In our system, the task of LSI suppression is achieved in two stages: first, a passive suppression stage and, second, an active digital cancellation stage, which eliminates the LSI (including multi-path components) in baseband via software signal processing.

The baseband digital samples at the input of a full-duplex relaying node (shown in Figure 3b) can be written as

$$y_r[n] = x_s[n] * h_{s-r}[n] + I_r[n - \tau'] + w_r[n], \quad (14)$$

where  $y_r[n]$  are the received samples. The goal here is to eliminate the looped SI ( $I_r$ ), which originates as

$$I_r[n] = x_r[n] * h_{r-r}[n], \quad (15)$$

because of simultaneous reception and forwarding of the relay node. Here  $x_r[n]$  are the retransmitted samples generated after re-encoding, and  $\bar{h}_{r-r}$  is the self-interference channel between relay transmitting and receiving ends. Since  $x_r[n]$  are already known at the relay node so by obtaining an estimate of  $\bar{h}_{r-r}$ , approximate looped SI samples can be generated as

$$\hat{I}_r[n] = x_r[n] * \hat{h}_{r-r}[n]. \quad (16)$$

After adjusting the delay  $\tau'$  due to front end hardware, and subtracting Equations (14) and (16) yields

$$y_{\text{res}}[n] = x_s[n] * \bar{h}_{s-r} + w_r[n] + x_r[n - \tau'] * \bar{e}_{r-r}. \quad (17)$$

In Equation (17),  $\bar{e}_{r-r}$  represent the error vector due to the difference in actually received self-interference  $I_r$ , and regenerated SI  $\hat{I}_r$ . Note that if the error is negligible, i.e.,  $\bar{e}_{r-r} \approx 0$ , the residual LSI is completely eliminated and the expression is reduced to

$$y_{\text{res}}[n] = x_s[n] * h_{s-r}[n] + w_r[n]. \quad (18)$$

In Equation (18), the right-hand side is the same as for received samples in a typical receiver operating in HD mode.

In practice,  $\bar{e}_{r-r}$  can be reduced to significantly small numbers but it is never zero. This is certainly due to the inaccuracies in channel estimate, non-linear behavior of the amplifier, and oscillator phase noise at the retransmitting relay

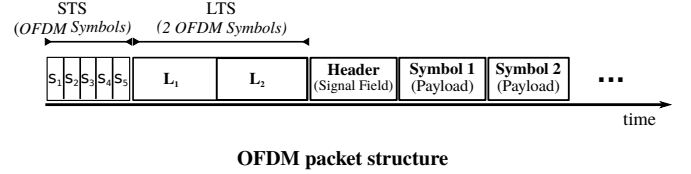


Figure 6. Overview of our OFDM-based packet structure. Each packet includes one short (STS) and two long training sequence (LTS) symbols for coarse and fine synchronization, and for channel estimation purposes. Followed by them is the signal field carrying the information of packet length, and then the actual payload symbols.

node. To keep the design simple and less complex, the latter two are not modeled in our system and left as potential future work. This work primarily focuses on the implementation of linear LSI cancellation in the digital domain. The impact of ignoring the other two parameters is further discussed and shown in Section VII.

#### A. Estimation of Looped SI Channel

To estimate the SI channel, we employed the time domain Least Squares (LS) estimation approach. The LS approach basically acquires the Channel Impulse Response (CIR) estimate  $\hat{h}_{r-r}$  through the LTS symbol embedded in the OFDM frame structure shown in Figure 6, during the training transmissions period, i.e.,  $x_s = 0$ .

From Equations (14) and (15), the received samples  $y_r$  during training transmissions are obtained as

$$y[n] = x_r[n] * h_{r-r}[n] + w[n], \quad (19)$$

i.e., only looped-back self-interference samples  $I_r$ . From (19), the received LTS samples can be written as

$$y_{LTS}^N = x_{LTS}^N * h_{r-r}^P + w_{LTS}^N, \quad (20)$$

where  $N$  represents the length of LTS samples and  $P$  indicates the number of channel taps, which typically corresponds to Cyclic Prefix (CP). For fixed and predefined  $x_{LTS}^N$  samples, the time-domain convolution in Equation (20) can be expressed as matrix multiplication, i.e.,

$$y_{LTS}^N = \mathbf{X}^{N \times P} \cdot h_{r-r}^P + w_{LTS}^N. \quad (21)$$

Here,  $\mathbf{X}^{N \times P}$  is the Toeplitz matrix of order  $N \times P$ , formed using the known transmitted LTS samples [24]. Also, since the LTS samples are fixed and known in advance, the matrix  $\mathbf{X}^{N \times P}$  can be precomputed and stored prior to the beginning of training transmissions.

The time domain least square estimate is thus obtained as

$$\hat{h}_{r-r}^P = \mathbf{X}^{N \times P \dagger} \cdot y_{LTS}^N, \quad (22)$$

where  $\mathbf{X}^{N \times P \dagger}$  is the Moore-Penrose (pseudo) inverse of  $\mathbf{X}^{N \times P}$  and  $y_{LTS}^N$  are the received LTS samples.

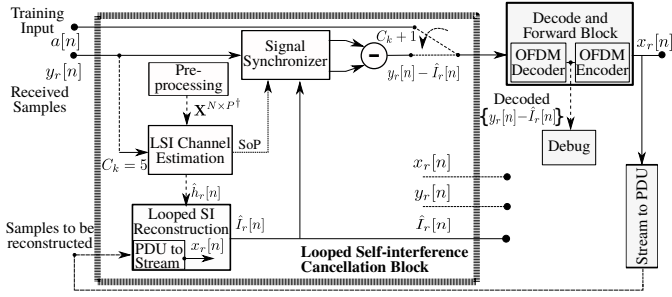


Figure 7. Detailed baseband level block diagram of our novel LSI suppression module for full-duplex relay implementation.

### B. Reconstruction of Looped SI

Reconstruction of the looped SI is similar to the equalization process but instead of equalizing the received samples, the known retransmitted samples  $x_r$  are equalized with the acquired channel estimate  $\hat{h}_{r-r}$ . In order to apply the channel impairment effects on reconstructed LSI samples, the estimated CIR is convolved with the known samples  $x_r$ , shown with Equation (16). As a result, the reconstructed self-interference samples  $\hat{I}_r$  innate the same channel properties as that carried by the received LSI samples  $I_r$ .

## V. IMPLEMENTATION DETAILS

For the performance evaluation, we implemented both HDR and FDR with DF relaying scheme in GNU Radio. We choose GNU Radio as the implementation platform because of its wide-spread use as a real-time signal processing framework and its ability to do rapid prototyping. Moreover, the GNU Radio Companion (GRC), a graphical tool for creating flow graph, allows to monitor – the real-time received/processed samples through visualization scopes in both time and frequency domains.

For the implementation of DF relaying scheme, we used GNU Radio’s OFDM blocks in the GRC with key parameters listed in Table I. The design of DF scheme based half-duplex relay is rather simple as it just needs to receive the packet from source, decode it, then re-encode and forward the packet to destination. However, for FDR, we have implemented a novel core block for the cancellation of looped-back self-interference in the GNU Radio framework. It is important to mention here that the GRC does not allow direct feedback of the streaming samples in a flow graph; which is the key requirement in FD relaying, necessary for the reconstruction of LSI. For this reason, all the re-encoded samples  $x_r$  are first converted into

a Protocol Data Unit (PDU) message, and then fed back to the looped SI cancellation block as illustrated in Figure 7.

### A. Looped SI Cancellation Block

The looped SI cancellation block first forwards the  $C_k + 1$  training packets within the DF relay node for the estimation of SI channel, and for stabilizing the sub-blocks such as signal synchronizer. In Figure 7,  $C$  represents the number of training packets and  $k$  is the process repetition interval. During the forwarding of training packets, the transmissions from the source are turned off until the relay switches to full-duplex relaying mode, as shown in Figure 7.

1) *Preprocessing*: The preprocessing block first performs the Inverse Fast Fourier Transform (IFFT) on the LTS symbol enclosed in the packet preamble, hence converting it into time-domain samples. Afterward, the obtained time-domain samples are used to create Toeplitz matrix  $\mathbf{X}^{N \times P}$ , and finally to calculate the Moore-Penrose (pseudo) inverse  $\mathbf{X}^{N \times P \dagger}$  of the Toeplitz matrix  $\mathbf{X}^{N \times P}$ , which is later used with received LTS samples  $y_{LTS}^N$  to compute the SI channel estimate. Here,  $N$  is same as the number of IFFT points and  $P$  is set to be half of CP, the values of each are listed in Tables I and II, respectively.

2) *SI Channel Estimation*: The estimation block operates only during the training transmissions. It first correlates the received samples  $y_r$  with the known LTS samples  $x_{LTS}^N$  to determine the Start-of-Packet (SoP). Once SoP is determined, it then extracts the received LTS samples  $y_{LTS}^N$  and uses them with  $\mathbf{X}^{N \times P \dagger}$  to compute the SI channel estimate  $\hat{h}_{r-r}$ .

3) *LSI Reconstruction*: The reconstruction block first converts the PDU message containing re-encoded samples  $x_r$  into streaming samples and then convolves them with the obtained SI channel estimate  $\hat{h}_{r-r}$  to produce approximate looped SI samples  $\hat{I}_r$ .

4) *Signal Synchronizer*: The synchronizer block synchronizes the reconstructed LSI samples  $\hat{I}_r$  with the received samples  $y_r$  during training transmissions. It calculates the delay introduced by the relay’s front ends, i.e., from Tx to Rx. Since the fed back known samples  $x_r$  arrive earlier compared to the received LSI samples, the synchronizer starts buffering the reconstructed samples and waits for an SoP indicator to release them. Also, the synchronizer block computes the required buffer length during the training session, i.e., no transmissions from the source. Once the buffer length is determined it does not change because the delay from relay Tx to Rx end remains the same.

Table I

KEY PARAMETERS OF THE EMPLOYED GNU RADIO’S OFDM BLOCK.

|                                     |                     |
|-------------------------------------|---------------------|
| Modulation                          | Q-PSK               |
| Number of Sub-Carriers              | 64                  |
| Pilots                              | 4                   |
| Data Carriers                       | 48                  |
| Cyclic Prefix Length                | 16                  |
| FFT/IFFT Size ( $N$ )               | 64 points           |
| Packet Preamble (STS + LTS) Symbols | (1 + 1) OFDM Symbol |
| Packet Header (3 B)                 | 1 OFDM Symbol       |

Table II

KEY PARAMETERS OF FD RELAY NODE.

|  |             |
|--|-------------|
| Training Packets ( $C$ )                 | 5           |
| Samples per Packet                       | 3520        |
| Number of Estimated Channel Taps ( $P$ ) | 8           |
| Sampling Frequency                       | 17.6 MHz    |
| OFDM Symbol Duration                     | 4.5 $\mu$ s |
| Cyclic Prefix Duration                   | 910 ns      |
| Estimable SI Channel Impulse Response    | 455 ns      |

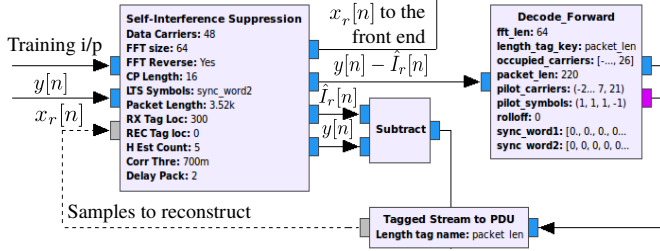


Figure 8. Screenshot of the most relevant blocks of our full-duplex relay implementation in GNU Radio Companion.

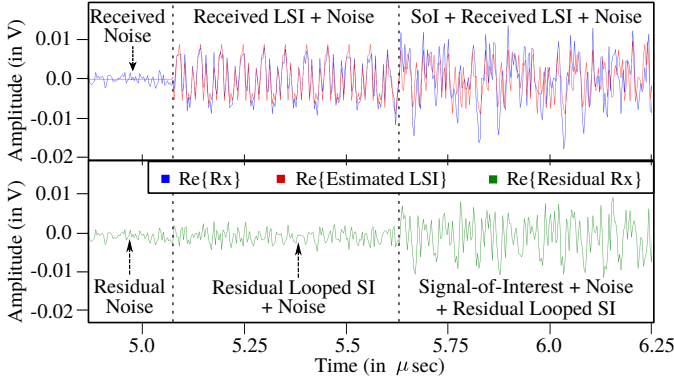


Figure 9. Snapshot of real-time LSI cancellation performance of our relay node under full-duplex mode with B-210 USRPs.

After synchronization, the reconstructed samples are subtracted from received samples and forwarded to the DF relaying block provided that the training transmission period is over. The decoded output of DF block is also fed to a debugger, to check whether a packet is correctly decoded.

Figure 8 shows the implemented LSI cancellation block and DF module in GNURadio. A screenshot of real-time looped SI cancellation with 0dBm transmit power level of the relay node is shown in Figure 9. For the sake of clarity, the figure only shows the cancellation performance with real samples, i.e., the in-phase component. The signals in blue, red and green are received (LSI & SoI), reconstructed LSI and (residual LSI & SoI), respectively.

### B. Passive Suppression

In our FDR systems, passive suppression is employed to suppress the direct/leaked SI signal, shown in Figure 2. As both Tx and Rx front ends are quite close, the looped-back SI signal is significantly stronger than the SoI arriving from a distant source, and if not suppressed to an extent, it can occupy the whole dynamic range of ADCs in the received signal process path. Therefore, the passive suppression stage is quite crucial. Different designs have been proposed for passive suppression [25]–[27], where an RF isolation of up to 73 dB is shown to be achieved.

In this work, we used a very basic RF isolation approach, which provides a passive suppression of approx. 52 dB. We placed a Balsa foam wrapped with aluminum foil between the transmit and receive antennas. Even though the approach does not sound efficient, but, considering the available resources

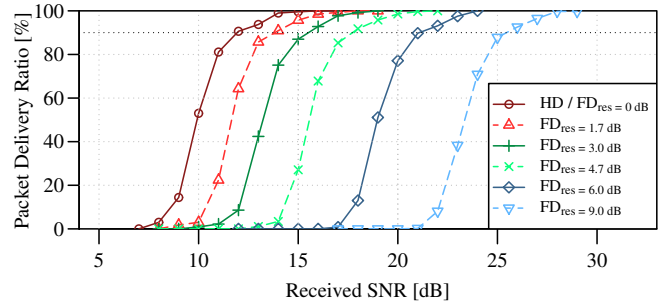


Figure 10. PDR against received SNR at the relay node in FD relaying mode for exceeding levels of residual LSI over the noise floor.

it has worked well enough to test, validate and evaluate the performance of our GNURadio-based FDR implementation.

## VI. SIMULATIVE EVALUATION

To draw a performance comparison between FD and HD relaying modes with decode and forward strategy, we conducted an extensive set of real-time simulations. We investigated the impact of the foremost parameter, i.e., the residual looped SI due to estimation error, on the performance of FD relaying mode, and computed Packet Delivery Ratio (PDR) under different levels of residual LSI. In our simulation setup, we transmitted 1000 OFDM-based packets with parameters listed in Table I, and measured the PDR based on received SNR. Each packet comprises of 250 B payload, 3 B header, and 4 B CRC. For each SNR point, the transmission of packets is repeated 20 times to obtain a 95 % confidence interval, which for the sake of clarity is not shown in the plots.

For the simulative evaluation of both FD and HD relaying system, we additionally implemented a 6-taps frequency-selective Rayleigh fading channels for both source-relay ( $h_{s-r}$ ) and relay-destination ( $h_{r-d}$ ) paths, and a linear 3-taps fading channel for looped SI channel ( $h_{r-r}$ ) in GNU Radio framework. To keep  $h_{r-r}$  more realistic, among the three taps first one is kept strongest as it maps the looped-back SI through the direct path, and the remaining are kept weak to model the multi-path effect.

Figure 10 illustrates the impact of residual looped-back SI on the performance of DF-based full-duplex relaying. In the plot, a PDR of 100 % means that all packets have been correctly detected and decoded, and the horizontal dashed line marks 90 % PDR level. In the figure, we observe that when residual LSI surpasses the noise floor i.e.,  $FD_{res}=1.7\text{dB}$  and above, more SNR is required to achieve 90 % PDR. This is rather expected because the LSI is nothing but interference for the SoI, which means any residual LSI above the noise floor, basically reduces the desired signal's SNR. Thus, in order to maintain high PDR performance, more SNR is required. Additionally, it is worth noticing here that the relation between required SNR and residual LSI is almost linear, e.g., from HD /  $FD_{res}=0\text{dB}$  to  $FD_{res}=1.7\text{dB}$  (i.e. 1.7 dB more LSI) an SNR gain of  $\approx 2\text{dB}$  is required to maintain the PDR level. This is due to the reason that the implemented LSI channel ( $h_{r-r}$ ) has linear behavior. However, this is not always the case especially

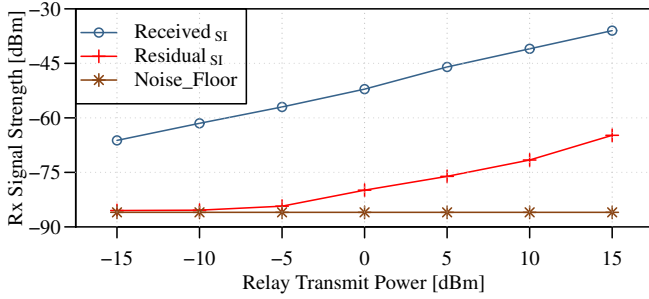


Figure 11. Looped SI suppression performance of the implemented FDR in the digital domain with increasing transmit power levels of the relay node.

when using the hardware with non-linear components like the amplifier, and it will be further discussed in the subsequent section. These simulation results also agree with our analytical findings Section III-C, where, for larger error vector magnitudes  $\|e_{r-r}\|^2$ , the normalized SNR in Equations (9) and (12) depreciates drastically. This intuitively means that for larger error, i.e., higher residual LSI, the performance drop is certainly expected, which can clearly be seen in the simulation results in terms of reduced PDR with increasing residual LSI.

## VII. PRACTICAL PERFORMANCE

For the practical performance evaluation of our DF-based FDR, we conducted experiments in our radio lab. In our experimental setup, we used three B210 USRP SDRs as transmitting, relaying, and receiving nodes. The S-R and S-D distances are 15 m and 30 m, respectively. In each transmission 46 packets are transmitted from the source node, and the process is repeated 20 times for every considered power level. A single packet includes 44 OFDM symbols out of which 3 symbols contribute towards the overhead (STS, LTS, and packet header). All relevant hardware-specific parameters are listed in Table III. It is worth mentioning here that since decoding delay in DF relaying scheme is the same regardless of HD or FD transmission mode, therefore, its impact is not studied in this work.

### A. Looped SI Suppression Performance

Figure 11 shows the looped SI suppression achieved in the digital domain for different transmit power levels of the relay node. The measured noise floor of B210 USRPs operating at a sampling frequency of 17.6 MHz is  $-86$  dBm. It can be seen in the figure that received LSI is suppressed to the receiver's noise floor for low transmit power level (up to  $-10$  dBm).

Table III  
HARDWARE-SPECIFIC PARAMETERS

|                             |               |
|-----------------------------|---------------|
| Carrier Frequency           | 868 MHz       |
| Receiver Noise Floor        | $-86$ dBm     |
| Source-Relay Distance       | 15 m          |
| Source-Destination Distance | 30 m          |
| RF LSI Isolation            | approx. 52 dB |
| Digital LSI Suppression     | up-to 32 dB   |

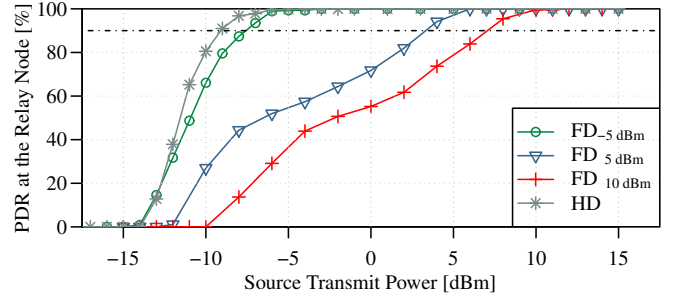


Figure 12. Experimentally measured PDR performances of DF based HDR and FDR implementations.

However, for higher transmit power levels, a gradual increase in the residual SI is observed due to the following reasons.

First, the obtained RF isolation is far from being perfect (reported as high as 73 dB) and with a higher transmit power level insufficient isolation becomes more obvious. By employing more sophisticated RF suppression techniques such as dual-port dual polarized slot coupled antenna or antenna separation through RF absorber along with orthogonal polarization, RF isolation can be greatly improved. Secondly, the implemented LSI suppression block does not model the non-linear behavior of the amplifier in the RF chain. For high transmit power levels, the non-linear factor added by the amplifier becomes more significant, resulting in increased levels of residual SI. By addressing the two mentioned factors, the residual SI can be further suppressed close to the receiver's noise floor, even at higher transmit powers of the relay node.

### B. Packet Delivery Ratio at the Relay Node: FDR vs HDR

In Figure 12, the achieved PDR at the relay node operating in both FD and HD mode is plotted for increasing transmit power level of the source node. Here, PDR 100 % means that all packets have been correctly detected and decoded at the receiver. The three FD mode curves in the plot represent the PDR obtained at different transmit power levels of the relay node (see legends subscript). It can be seen that the PDR with both  $FD_{-5\text{ dBm}}$  and HD is relatively similar. There is a roughly 1 dB difference in the performance certainly due to non-negligible residual LSI. Also, the PDR performances with  $FD_{5\text{ dBm}}$  and  $FD_{10\text{ dBm}}$  is much worse, both achieve 100 % PDR at higher source transmit power levels. This is due to the reason that when more transmitter gain is applied at relay node, i.e.,  $FD_{5\text{ dBm}}$  and  $FD_{10\text{ dBm}}$ , the increased residual LSI as a result, raises the noise-plus-interference level for SoI arriving from source node, hence more power is needed from source to overcome this increased noise floor, and to maintain 100 % PDR. Additionally, the linear SNR versus residual LSI behavior that we observed in the simulative evaluation section is no longer valid here, clearly due to the non-linear nature of the residual LSI – in particular at  $FD_{5\text{ dBm}}$  and  $FD_{10\text{ dBm}}$ .

Figure 13 demonstrates the required source transmit power levels for a given relay transmit power to maintain a PDR of 90 % at the relay node. Ideally, this plot should have been a straight horizontal line, however, a ramp-like function here is

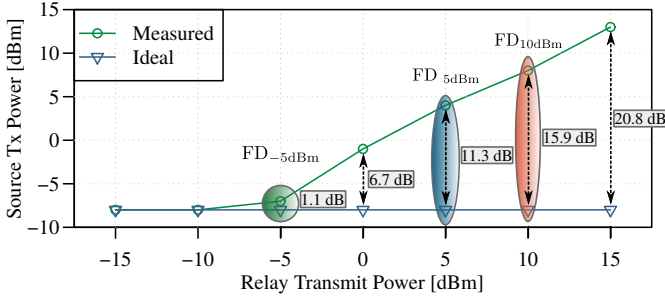


Figure 13. Required source transmit power levels to maintain PDR of 90% for a given relay transmit power. The circled points highlight the 90% PDR values in Figure 12.

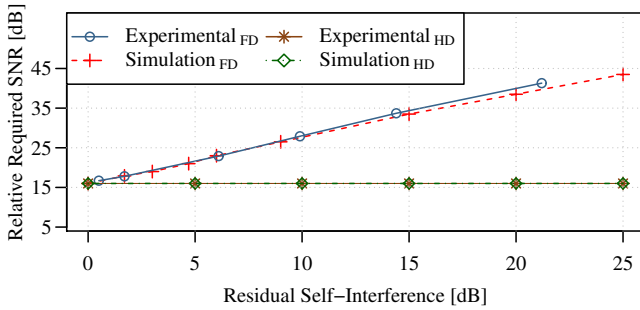


Figure 14. Relative required SNR to maintain 100% PDR at the relay node in both simulations and experimental studies.

due to the increasing levels of residual LSI at higher relay transmit power. This, as a result, raises the overall noise-plus-interference level for SoI and more transmit power is required from the source to retain the desired 90% PDR.

### C. Impact of Residual LSI on PDR

Figure 14 demonstrates the PDR performance comparison of simulations with experiments over increasing residual LSI. In the figure, it can be seen that the relative required SNR to maintain 100% PDR in both simulations and experiments for the HDR case is rather similar, irrespective of the residual LSI strength. This is intuitive, as there is no impact of LSI in HDRs because of time separate reception and forwarding. Nevertheless, for FDRs, the relative required SNR in the experiments starts deviating from the simulations after 10 dB residual LSI and requires additional SNR to maintain 100% PDR. This is because of the reason that unlike simulations where the residual LSI was linear in nature, the residual LSI in experiments also includes the non-linear fraction of the LSI, especially at higher power transmissions of the relay node. This non-linear fraction of the LSI exists due to the non-linear behavior of the amplifier in the transmitting chain, which only strengthens with increasing gain values. Additionally, the high Peak-to-Average Power Ratio (PAPR) in OFDM further aggravates this non-linear LSI situation, and eventually have a stronger impact on the decoding of packets, as compared to simple linear residual LSI. These results further indicate the impact of the non-linear fraction of residual LSI on the performance of FDRs, which certainly needs to be suppressed

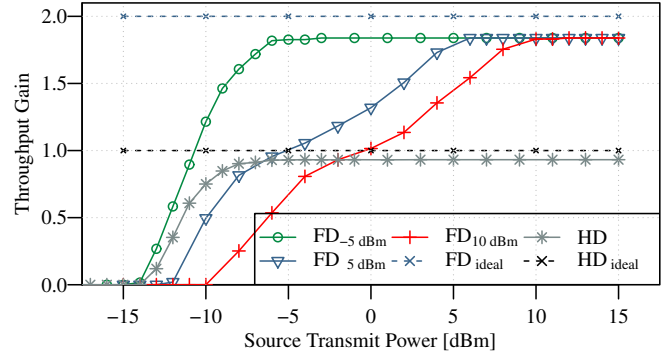


Figure 15. Achieved throughput gains with FD relaying over HDR at different transmit power levels of the relay node.

for optimal performance gains.

### D. Throughput Gain: FDR vs HDR

Figure 15 depicts the throughput gain of FD relaying over HDR system in our described experimental setup. To keep the training transmission overhead to a minimum, the training packets  $C$  are fixed to 5. Ideally, the throughput gain with FDR should be twice of HDR, however, after considering both packet and training transmission overheads, a maximum throughput gain of  $1.8\times$  is measured with  $FD_{-5dBm}$ . This is still a nearly two-fold increase in throughput gain with FDR over HD relaying. The figure also demonstrates that at high transmit power level of the relay node, which results in residual LSI, reduces the throughput gain considerably as compared to the throughput gain achieved at low transmit power level to which the residual LSI is almost eliminated. These results clearly highlight the strict requirement of residual LSI suppression to the receiver's noise floor in FDRs, to achieve maximum throughput gains, especially at higher transmit power levels of the relay node.

## VIII. CONCLUSION

In this paper, we presented a novel SDR-based real-time Full-Duplex (FD) Decode and Forward (DF) relay implementation in GNU Radio, which also allows to monitoring the real-time Looped Self-Interference (LSI) cancellation in both time and frequency domains. To the best of our knowledge, this is the first lab-ready GPP-based FD relaying system. Our FDR implementation prototype is based on open-source GNU Radio framework, and with slight modifications, it can be extended to work with any OFDM-based wireless system. We validated the system in a series of experiments, also comparing the achieved results with analytical and simulation results. We can report that we were able to measure almost twice the throughput using our FDR compared to a Half-Duplex Relay (HDR) when LSI is fully suppressed. We further studied the effects of residual LSI on the full-duplex relaying performance. Even though there is a need for more advanced RF isolation between the two antennas, our system is able to achieve very good performance results in the used lab setup.

## REFERENCES

- [1] 3GPP, "Further advancements for E-UTRA physical layer aspects," 3GPP, TR 36.814 V9.0.0 (2010-03), 3 2010.
- [2] "Local and metropolitan area networks," IEEE, Standard P802.16j-06/026r4, 5 2007.
- [3] Z. Zhang, K. Long, A. V. Vasilakos, and L. Hanzo, "Full-duplex wireless communications: Challenges, solutions, and future research directions," *Proceedings of the IEEE*, vol. 104, no. 7, pp. 1369–1409, 2016.
- [4] A. Sahai, G. Patel, and A. Sabharwal, "Pushing the limits of full-duplex: Design and real-time implementation," arXiv, cs.NI 1107.0607, 7 2011. [Online]. Available: <http://arxiv.org/abs/1107.0607>
- [5] D. Bharadia, E. McMillin, and S. Katti, "Full Duplex Radios," *ACM SIGCOMM Computer Communication Review (CCR)*, vol. 43, no. 4, pp. 375–386, 10 2013.
- [6] S. Ashutosh, S. Philip, G. Dongning, W. B. Daniel, R. Sampath, and W. Risto, "In-Band Full-Duplex Wireless: Challenges and Opportunities," *IEEE Journal on Selected Areas in Communications*, vol. 32, no. 9, pp. 1637–1652, 9 2014.
- [7] E. Ahmed and A. M. Eltawil, "All-digital self-interference cancellation technique for full-duplex systems," *IEEE Transactions on Wireless Communications*, vol. 14, no. 7, pp. 3519–3532, 7 2015.
- [8] H. Zhuang, J. Li, W. Geng, and X. Dai, "Duplexer design for full-duplex based wireless communications," *China Communications*, vol. 13, no. 11, pp. 1–13, 2016.
- [9] K. Dani, T. Joose, T. Matias, H. Timo, C. Yang-Seok, A. Lauri, T. Shilpa, and V. Mikko, "Full-duplex mobile device: pushing the limits," *IEEE Communications Magazine*, vol. 54, no. 9, pp. 80–87, 9 2016.
- [10] J. Zhou, N. Reiskarimian, J. Diakonikolas, T. Dinc, T. Chen, G. Zussman, and H. Krishnaswamy, "Integrated Full Duplex Radios," *IEEE Communications Magazine*, vol. 55, no. 4, pp. 142–151, 2017.
- [11] M. S. Amjad, H. Nawaz, K. Ozsoy, O. Gurbuz, and I. Tekin, "A Low-Complexity Full-Duplex Radio Implementation With a Single Antenna," *IEEE Transactions on Vehicular Technology*, vol. 67, no. 3, pp. 2206–2218, 3 2018.
- [12] M. S. Amjad and F. Dressler, "Experimental Insights on Software-based Real-Time SI Cancellation for In-Band Full Duplex DF Relays," in *IEEE International Conference on Communications (ICC 2019)*. Shanghai, China: IEEE, 5 2019.
- [13] J. Laneman, D. Tse, and G. Wornell, "Cooperative Diversity in Wireless Networks: Efficient Protocols and Outage Behavior," *IEEE Transactions on Information Theory*, vol. 50, no. 12, pp. 3062–3080, 12 2004.
- [14] B. Rankov and A. Wittneben, "Spectral efficient protocols for half-duplex fading relay channels," *IEEE Journal on Selected Areas in Communications*, vol. 25, no. 2, pp. 379–389, 2 2007.
- [15] J. Jiao, X. Jia, M. Zhou, M. Xie, and Q. Cao, "Full-duplex massive MIMO AF relaying system with low-resolution ADCs under ZFT/ZFR scheme," in *2nd IEEE Advanced Information Technology, Electronic and Automation Control Conference (IAEAC 2017)*. Chongqing, China: IEEE, 3 2017, pp. 2024–2028.
- [16] Q. Li, S. Feng, X. Ge, G. Mao, and L. Hanzo, "On the Performance of Full-Duplex Multi-Relay Channels With DF Relays," *IEEE Transactions on Vehicular Technology*, vol. 66, no. 10, pp. 9550–9554, 10 2017.
- [17] L. Elsaid, M. Ranjbar, N. Raymondi, D. Nguyen, N. Tran, and A. Mahamadi, "Full-Duplex Decode-and-Forward Relaying: Secrecy Rates and Optimal Power Allocation," in *85th IEEE Vehicular Technology Conference (VTC2017-Spring)*. Sydney, Australia: IEEE, 6 2017.
- [18] F. H. Gregorio, G. J. Gonzalez, J. Cousseau, T. Riihonen, and R. Wichman, "RF Front-End Implementation Challenges of In-band Full-Duplex Relay Transceivers," in *European Wireless Conference (EW 2016)*. Oulu, Finland: IEEE, 5 2016.
- [19] T.-C. Chen, Y.-C. Chen, M.-K. Chang, and G.-C. Yang, "The Impact of Loopback Channel Estimation Error on Performance of Full-Duplex Two-Way AF Relaying Communication Systems," in *85th IEEE Vehicular Technology Conference (VTC2017-Spring)*. Sydney, Australia: IEEE, 6 2017.
- [20] D. Bharadia and S. Katti, "Fastforward: Fast and constructive full duplex relays," *ACM SIGCOMM Computer Communication Review (CCR)*, vol. 44, no. 4, pp. 199–210, 2015.
- [21] S. Mohammad, Z. Ammar, and Hussein, Alnuweiri and Mohamed-Slim, Alouini, "Maximizing Expected Achievable Rates for Block-Fading Buffer-Aided Relay Channels," *IEEE Transactions on Wireless Communications*, vol. 15, no. 9, pp. 5919–5931, 9 2016.
- [22] Q. Deli, "Effective Capacity of Buffer-Aided Full-Duplex Relay Systems With Selection Relaying," *IEEE Transactions on Communications*, vol. 64, no. 1, pp. 117–129, 1 2016.
- [23] M. R. Mohsen and Z. Nikola, "Buffer-aided relaying for the two-hop full-duplex relay channel with self-interference," *IEEE Transactions on Wireless Communications*, vol. 17, no. 1, pp. 477–491, 1 2018.
- [24] M. S. Amjad and O. Gurbuz, "Linear Digital Cancellation with Reduced Computational Complexity for Full-Duplex Radios," in *IEEE Wireless Communications and Networking Conference (WCNC 2017)*. San Francisco, CA: IEEE, 3 2017.
- [25] M. Jain, J. I. Choi, T. Kim, D. Bharadia, S. Seth, K. Srinivasan, P. Levis, S. Katti, and P. Sinha, "Practical, Real-time, Full Duplex Wireless," in *17th ACM International Conference on Mobile Computing and Networking (MobiCom 2011)*. Las Vegas, NV: ACM, 9 2011, pp. 301–312.
- [26] E. Everett, A. Sahai, and A. Sabharwal, "Passive self-interference suppression for full-duplex infrastructure nodes," *IEEE Transactions on Wireless Communications*, vol. 13, no. 2, pp. 680–694, 2014.
- [27] H. Nawaz and I. Tekin, "Three dual polarized 2.4GHz microstrip patch antennas for active antenna and in-band full duplex applications," in *16th Mediterranean Microwave Symposium (MMS 2016)*. Abu Dhabi, United Arab Emirates: IEEE, 11 2016.



**Muhammad Sohaib Amjad** ([amjad@ccs-labs.org](mailto:amjad@ccs-labs.org)) joined the Distributed Embedded Systems Group (CCS Labs) as a Researcher/PhD student in 2017. He received his MSc in electronics engineering from Sabanci University, Istanbul, Turkey in 2016, and his BSc in electrical engineering from Air University, Islamabad, Pakistan in 2011. His research focuses on topics related to wireless communication physical layer and signal processing, more specifically full-duplex wireless communication, mmWave communication, and vehicular visible light communication (V-VLC). He is an IEEE COMSOC student member and serves as a reviewer for manuscripts in the field of wireless communications.



**Falko Dressler** ([dressler@ccs-labs.org](mailto:dressler@ccs-labs.org)) is full professor of computer science and chair for Distributed Embedded Systems at the Heinz Nixdorf Institute and the Dept. of Computer Science, Paderborn University. He received his M.Sc. and Ph.D. degrees from the Dept. of Computer Science, University of Erlangen in 1998 and 2003, respectively. Dr. Dressler is associate editor-in-chief for Elsevier Computer Communications as well as an editor for journals such as IEEE/ACM Trans. on Networking, IEEE Trans. on Network Science and Engineering, Elsevier Ad Hoc Networks, and Elsevier Nano Communication Networks. He has been chairing conferences such as IEEE INFOCOM, ACM MobiSys, ACM MobiHoc, IEEE VNC, IEEE GLOBECOM, and many others. He has been an IEEE Distinguished Lecturer as well as an ACM Distinguished Speaker. Dr. Dressler is an IEEE Fellow as well as an ACM Distinguished Member.